P-Coligand Tuning of the Haptotropic Metal Migration in Phenanthrene Chromium Complexes

Oliver Joistgen,[†] Anja Pfletschinger,[‡] Jan Ciupka,[‡] Michael Dolg,[‡] Martin Nieger,[§,#] Gregor Schnakenburg,[§] Roland Fröhlich,[⊥] Olga Kataeva,[⊥] and Karl Heinz Dötz*[,†]

Kekulé-Institut für Organische Chemie und Biochemie, Rheinische Friedrich-Wilhelms-Universität, Bonn, Gerhard-Domagk-Strasse 1, D-53121 Bonn, Germany, Institut für Theoretische Chemie, Universität zu Köln, Greinstrasse 4, D-50939 Köln, Germany, Institut für Anorganische Chemie, Rheinische Friedrich-Wilhelms-Universität, Bonn, Gerhard-Domagk-Strasse 1, D-53121 Bonn, Germany, Laboratory of Inorganic Chemistry, Department of Chemistry, University of Helsinki, FIN-00014, Finland, and Organisch-Chemisches Institut, Universität Münster, Corrensstrasse 40, D-48149 Münster, Germany

Received January 26, 2009

The hydroquinoid phenanthrene $Cr(CO)_3$ complex **1**, directly accessible from the benzannulation of pentacarbonyl[(methoxy)-1-naphthylcarbene]chromium with 3-hexyne as the kinetically favored isomer, and its thermodynamically stable haptotropomer **2** undergo a photoinduced substitution of one CO ligand for phosphines and phosphites PR_3 (R = Me, OMe, Ph, OPh) to give (η^6-phenanthrene)$Cr(CO)_2PR_3$ complexes **3**−**10**. Upon warming chromium complexes **3**−**6**, a haptotropic metal migration affords regioisomers **7**−**10** in up to 79% yield bearing the chromium fragment coordinated to the terminal unsubstituted phenanthrene ring. The rearrangements have been monitored by IR and NMR spectroscopy. Kinetic NMR experiments in noncoordinating solvents such as hexafluorobenzene reveal first-order kinetics in line with an intramolecular metal shift along the extended π-system. The metal migration can be tuned by the *P*-based coligand as demonstrated by rate constants differing by 2 orders of magnitude and by barriers of activation differing by 15 kJ mol^{-1}, respectively. A quantitative analysis (QALE) of these ligand effects suggests that the rearrangement is controlled by both electronic and steric properties of the *P*-coligand. The molecular structures of the complexes **3**, **4**, and **6**−**10** were established by single-crystal X-ray analysis. Quantum chemical DFT calculations provide a mechanistic rationale of the haptotropic migration in naphthalene and phenanthrene $Cr(CO)_2PR_3$ complexes.

Introduction

Transition metal complexes with unsaturated ligands such as polycyclic arenes or oligoenes offering more than one coordination site are able to undergo a metal shift along the π-skeleton. This rearrangement is usually referred to as a haptotropic metal migration and has been studied for several metals as well as for different ligand systems.[1] Although this phenomenon is known for several kinds of metal complexes, it has been most intensively studied in tricarbonyl(η^6-arene)chromium complexes due to their easy accessibility via $Cr(CO)_3$ transfer procedures. Early research focused mainly on $\eta^6-\eta^6$-rearrangements in tricarbonyl(η^6-naphthalene)chromium complexes[2] but more recently has been extended to fused arenes such as phenanthrene,[3] naphthobenzofuran, and naphthobenzothiophene.[4] The mechanism of the haptotropic metal migration has been investigated using experimental and theoretical methods. EHMO and, more recently, DFT calculations suggested that the metal shift in tricarbonyl(η^6-naphthalene)chromium complexes does not follow the least motion pathway across the ring junction but rather occurs along the periphery of the naphthalene system with a η^4-trimethylene methane complex type transition state.[1a,d,e,5] A similar metal migration principle has been revealed for tricarbonyl(η^6-phenanthrene)chromium[3,6] and complexes with

* Corresponding author. Fax: (+49) 228 735813. E-mail: doetz@uni-bonn.de.

† Kekulé-Institut für Organische Chemie und Biochemie, Rheinische Friedrich-Wilhelms-Universität.

‡ Universität zu Köln.

§ Institut für Anorganische Chemie, Rheinische Friedrich-Wilhelms-Universität.

University of Helsinki.

⊥ Universität Münster.

(1) For reviews see: (a) Albright, T. A.; Hofmann, P.; Hoffmann, R.; Lillya, C. P.; Dobosh, P. A. *J. Am. Chem. Soc.* **1983**, *105*, 3396–3411. (b) Kündig, E. P.; Desorby, V.; Grivet, C.; Spichiger, S. *Organometallics* **1987**, *6*, 1173. (c) Morris, M. J. In *Comprehensive Organometallic Chermistry II*; Abel, E. W., Stone, F. G. A., Wilkinson, G. Eds.; Pergamon Press: New York, 1995; Vol. 5, pp 501−504. (d) Oprunenko, Y. F. *Russ. Chem. Rev.* **2000**, *69*, 683–704. (e) Dötz, K. H.; Stendel. J., Jr. In *Modern Arene Chemistry*; Astruc, D. Eds.; Wiley-VCH: Weinheim, Germany, 2002. (f) Dötz, K. H.; Wenzel, B.; Jahr, H. C. Chromium-Templated Benzannulation and Haptotropic Metal Migration. *Top. Curr. Chem.* **2004**, *248*, 63–103. (g) Gridnev, I. D. *Coord. Chem. Rev.* **2008**, *252*, 1798–1818.

(2) (a) Cunningham, S. D.; Öfele, K.; Willeford, B. *J. Am. Chem. Soc.* **1983**, *105*, 3724. (b) Dötz, K. H.; Dietz, R. *Chem. Ber.* **1977**, *110*, 1555. (c) Dötz, K. H.; Stinner, C. *Tetrahedron: Asymmetry* **1997**, *8*, 1751–1756. (d) Kündig, E. P.; Peret, C.; Spichiger, S.; Bernadinelli, G. *J. Organomet. Chem.* **1985**, *286*, 183–200. (e) Kriss, R. U.; Treichel, P. M. *J. Am. Chem. Soc.* **1986**, *108*, 853–855. (f) Oprunenko, Y. F.; Malyugina, S. G.; Ustynyuk, Y. A.; Ustynyuk, N. A.; Kravtsov, D. N. *J. Organomet. Chem.* **1988**, *338*, 357–368.

(3) (a) Dötz, K. H.; Stendel, J., Jr.; Müller, S.; Nieger, M.; Ketrat, S.; Dolg, M. *Organometallics* **2004**, *24*, 3219–3228. (b) Dötz, K. H.; Stendel, J., Jr.; Nieger, M. *Z. Anorg. Allg. Chem.* **2009**, *635*, 221–237.

(4) (a) Dötz, K. H.; Jahr, H. C.; Nieger, M. *J. Organomet. Chem.* **2002**, *641*, 185–194. (b) Schneider, J. F.; Nättinen, K.; Lewall, B.; Nieger, M.; Niecke, E.; Dötz, K. H. *Eur. J. Org. Chem.* **2005**, 1541–1560.

(5) (a) Ref 1a. (b) Oprunenko, Y. F.; Akhmedov, N. G.; Laikov, D. N.; Malyugina, S. G.; Mstislavsky, V. I.; Roznyatovsky, V. A.; Ustynyuk, Y. A.; Ustynyuk, N. A. *J. Organomet. Chem.* **1999**, *583*, 136–145.

(6) Dolg, M.; Müller, S.; Ketrat, S. *J. Phys. Chem. A* **2007**, *111*, 6094–6102.

10.1021/om900057a CCC: $40.75
Publication on Web 05/08/2009

Scheme 1. Synthesis of Kinetic and Thermodynamic Tricarbonyl(η^6-phenanthrene)chromium Complexes 1 and 2

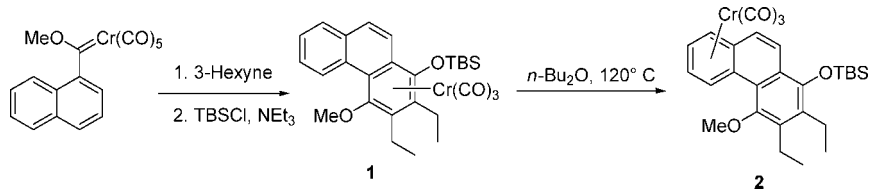

more extended arene platforms.[7] A competitive scenario for a metal transfer in fused arenes from one ring to another may be based on an intermolecular, a dissociative, or a decomplexation/recomplexation mechanism depending on the reaction conditions used for the regioisomerization. High concentrations and elevated temperatures favor an intermolecular mechanism in which the chromium fragment is directly transferred from one arene to another, while a dissociative and a decomplexation/recomplexation mechanism are supported by coordinating solvents in which the metal fragment is completely disconnected from the arene and transferred via solvent-stabilized intermediates to the other coordination site or to another arene.[8] To preserve the chiral information implemented in enantiopure planar-chiral tricarbonyl(η^6-arene)chromium complexes, noncoordinating or weakly coordinating solvents and only moderate temperatures should be applied, which allow for *intra*molecular haptotropic rearrangements.[2b]

We aim at a systematic tuning of the haptotropic metal migration along polycyclic arene platforms following different approaches. A variation of the arene substitution pattern and thus of the electronic properties of the coordinated π-ligand in hydroquinoid (η^6-naphthalene)-[9] and (η^6-phenanthrene)-$Cr(CO)_3$ complexes[3] has been demonstrated to allow for a control of the haptotropic migration rates.[3] Alternatively, the metal shift has been governed by an adjustment of the electronic properties of the metal fragment by tuning the coligand sphere as shown for enantiopure planar-chiral tricarbonyl(η^6-naphthalene)chromium complexes,[10] which resulted in the elaboration of a stereospecific organometallic switch with retention of configuration.[11] More recently, a $\sigma-\pi$-switch was developed based on an azaborine chromium complex.[12] In this paper, we concentrate on the influence of the chromium coligand sphere and report on the haptotropic migration in phenanthrene $Cr(CO)_3$ complexes controlled by phosphines and phosphites differing in their electronic and steric properties.

Results and Discussion

Synthesis of Phenanthrene $Cr(CO)_2PR_3$ Complexes. The chromium-templated benzannulation of an arylcarbene ligand by an alkyne and carbon monoxide allows for a regiospecific metal labeling of an aromatic ring in fused arenes.[13] Reaction of pentacarbonyl[methoxy(1-naphthylcarbene)]chromium with 3-hexyne, carried out under kinetic control, affords exclusively the [(η^6-1,2,3,4,4a,10a)-phenanthrene]chromium complex **1**, which, upon warming, rearranges nearly quantitatively to its thermodynamic haptotropomer **2** (Scheme 1).[3]

Scheme 2. Synthesis of P-Based Phenanthrene Chromium Complexes 3−10

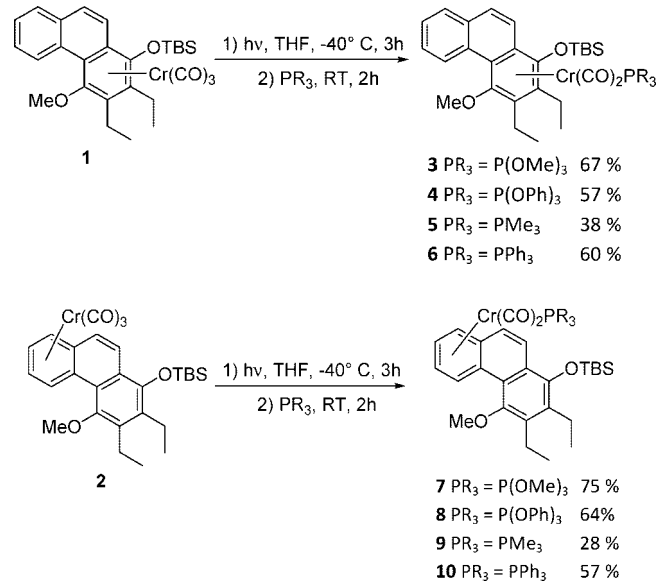

For the synthesis of the chromium phosphine and phosphite complexes **3−10** tricarbonyl chromium complexes **1** and **2** have been subjected to a photoinduced decarbonylation in tetrahydrofuran at low temperature.[14] The coordinatively unsaturated dicarbonylchromium complex intermediate is stabilized by tetrahydrofuran to give a labile dicarbonyl(THF)chromium complex. Subsequent substitution of the labile tetrahydrofuran ligand for trimethylphosphite, trimethylphosphine, triphenylphosphite, and triphenylphosphine at room temperature afforded phosphine and phosphite complexes **3−10** in 28−75% yield (Scheme 2).

Each pair of phosphine or phosphite chromium complexes represents a pair of haptotropomers in which the complexes **3−6** are the kinetically more stable isomers. In order to evaluate the role of the *P*-ligand in the metal migration, complexes **3−6** were

(7) (a) Sola, M.; Robles, J.; Jimenez-Halla, J. O. C. *J. Phys. Chem. A* **2008**, *112*, 1202. (b) Sola, M.; Robles, J.; Jimenez-Halla, J. O. C. *Organometallics* **2008**, *27*, 5230–5240.

(8) For examples of a metal transfer from one arene ring to another in biphenyl and diphenylether $Cr(CO)_3$ complexes at considerably higher temperatures (140−205 °C) suggesting an intermolecular decomplexation−recomplexation pathway, see: (a) Oprunenko, Y. F.; Shapshnikova, I. A.; Ustynyuk, Y. A. *Metalloorg. Khim.* **1991**, *4*, 1377–1390. (b) Rose-Munch, F.; Rose, E.; Semra, A. *J. Chem. Soc., Chem. Commun.* **1986**, 1108–1109.

(9) Dötz, K. H.; Szesni, N.; Nieger, M.; Nättinen, K. *J. Organomet. Chem.* **2003**, *671*, 58–74.

(10) (a) Dötz, K. H.; Jahr, H. C.; Nieger, M. *Chem. Eur. J.* **2005**, *11*, 5333–5342. (b) Dötz, K. H.; Jahr, H. C. *Chem. Rec.* **2004**, *4*, 61–71.

(11) Dötz, K. H.; Jahr, H. C.; Nieger, M. *Chem. Commun.* **2003**, 2866–2867.

(12) Pan, J.; Kampf, J. W.; Ashe, A. J., III. *Organometallics* **2006**, *25*, 197–202.

(13) For reviews see: (a) Dötz, K. H. *Angew. Chem., Int. Ed. Engl.* **1984**, *23*, 587–608; *Angew. Chem.* **184**, *96*, 573−594. (b) Wulff, W. D. In *Comprehensive Organometallic Chemistry*; Abel, E. W., Stone, F. G. A., Wilkinson, G. Eds.; Pergamon Press: Oxford, 1995, Vol. 12, pp 469−547. (c) Minatti, A.; Dötz, K. H. *Top. Organomet. Chem.* **2004**, *13*, 123–156. (d) Dötz, K. H.; Stendel, J., Jr. In *Modern Arene Chemistry*; Astruc, D. Ed.; Wiley-VCH: Weinheim (Bergstr.), 2002; pp 250−296. (e) Dötz, K. H.; Tomuschat, P. *Chem. Soc. Rev.* **1999**, *28*, 187–198.

(14) (a) Strohmeier, W. *Angew. Chem., Int. Ed. Engl.* **1964**, *11*, 730–737; *Angew. Chem.* **1964**, *21*, 873−881. (b) Cais, M.; Kaftory, M.; Kohn, D. H.; Tatarsky, D. *J. Organomet. Chem.* **1979**, *184*, 103–112. (c) For an oxidative displacement of a CO ligand by a phosphine or phosphite in arene complexes, see: Rose-Munch, F.; Susanne, C.; Renard, C.; Rose, E.; Vaisserman, J. *J. Organomet. Chem.* **1996**, *519*, 253–259.

Table 1. Thermo-induced Haptotropomerization of Complexes 3−6, Monitored via IR

complex	PR_3	A_1 [cm^{-1}][a]	B_1 [cm^{-1}][a]	T [°C][b]	time [min][b]	yield [%][b]
3	$P(OMe)_3$	1897	1849			
7	$P(OMe)_3$	1907	1859	120	90	64
4	$P(OPh)_3$	1903	1853			
8	$P(OPh)_3$	1922	1870	90	75	79
5	PMe_3	1878	1830			
9	PMe_3	1897	1847	90	30	23
6	PPh_3	1878	1830			
10	PPh_3	1901	1857	90	60	54

[a] Measured in petroleum ether at room temperature. [b] Reaction conditions and yields for the thermally induced metal migration.

Scheme 3. Thermo-induced Haptotropomerization of Complexes 3−6

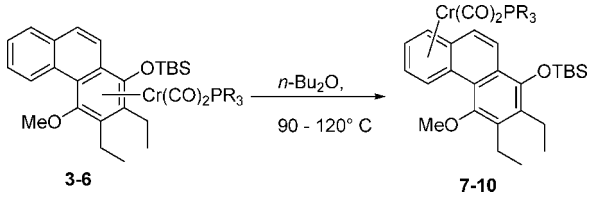

Table 2. ^{1}H NMR Coordination Shifts in Haptotropomers 7−10

complex	H5 [ppm]	H6/H7 [ppm]	H8 [ppm]
7[a]	7.50	5.28/5.19	5.62
8[a]	7.00	4.63/4.41	4.95
9[b]	7.21	5.23/5.06	5.94
10[a]	7.17	4.96/4.65	5.06

[a] In $CDCl_3$. [b] In CD_2Cl_2.

subjected to a thermo-induced isomerization in di-*n*-butyl ether at temperatures between 90 and 120 °C over a period of 30 − 90 min to form the thermodynamic haptotropomers **7**−**10**. The metal migration was monitored by infrared spectroscopy focusing on the hypsochromic shift of the A_1 bands of the carbonyl ligands (Table 1). The reaction was stopped when the starting material was consumed or when rapid decomposition was indicated by formation of $Cr(CO)_6$. After chromatographic workup the thermodynamic haptotropomers **7**−**10** were isolated in 23−79% yield. The low yield of the trimethylphosphine complex **9** was due to rapid decomposition, which forced us to stop the reaction after 30 min (Scheme 3). The coordination of the chromium fragment to the unsubstituted terminal benzene ring is further demonstrated by the characteristic upfield shift of the benzene hydrogen atoms in the ^{1}H NMR spectra of complexes **7**−**10** (Table 2).

Molecular Structures. The molecular structures of the phenanthrene complexes were determined by single-crystal X-ray crystallography (Figures 1−7). Suitable crystals of complexes **3**, **4**, and **6**−**10** were obtained by slow evaporation of the solvent (dichloromethane or diethyl ether). All arene platforms deviate from planarity with torsion angles of 8.1−12° at the inner phenanthrene bay induced by the methoxy substituent. No obvious correlation of the conformation of the chromium tripod with the nature of the *P*-ligand is observed. In the majority of the complexes the relative position of the Cr−P bond is eclipsed to one of the coordinated arene carbon atoms. In the kinetically favored $P(OMe)_3$ complex **3** the Cr−P bond is eclipsed to C4 and adopts a position away from the bulky silyl group. In contrast, in complexes **4** and **6**, revealing a staggered conformation with respect to the carbon atoms C4 and C4a, the PPh_3 and the $P(OPh)_3$ ligands are orientated above the silyl group. In the thermodynamically favored haptotropomers **7**, **9**, and **10** the $P(OMe)_3$, PMe_3, and PPh_3 ligands lie

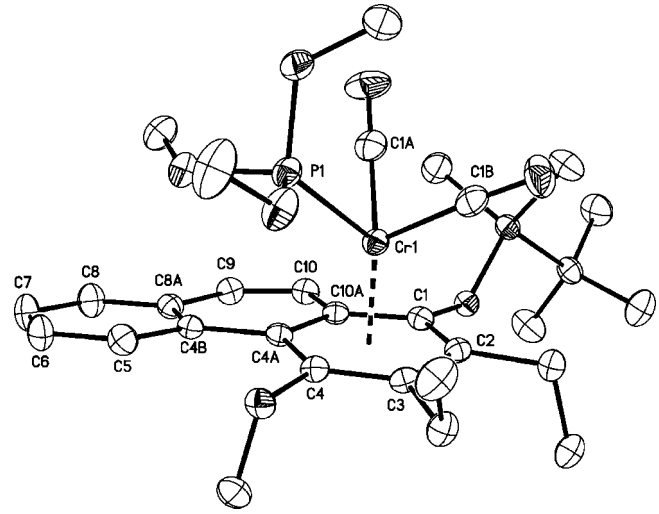

Figure 1. Molecular structure of $P(OMe)_3$ complex **3**. Hydrogen atoms have been omitted for clarity. Displacement parameters are drawn at the 50% probability level. Selected bond distances [Å]: Cr1−P1 2.2275(7), Cr1−C1 2.236(2), Cr1−C2 2.225(2), Cr1−C3 2.263(2), Cr1−C4 2.238(2), Cr1−C4A 2.293(2), Cr1−C10A 2.293(2), Cr1−Z_{Ar} 1.753(2), Cr1−C1A 1.821(3), Cr1−C1B 1.818(3). Selected torsion angle [deg]: C4−C4A−C4B−C5 9.6(4).

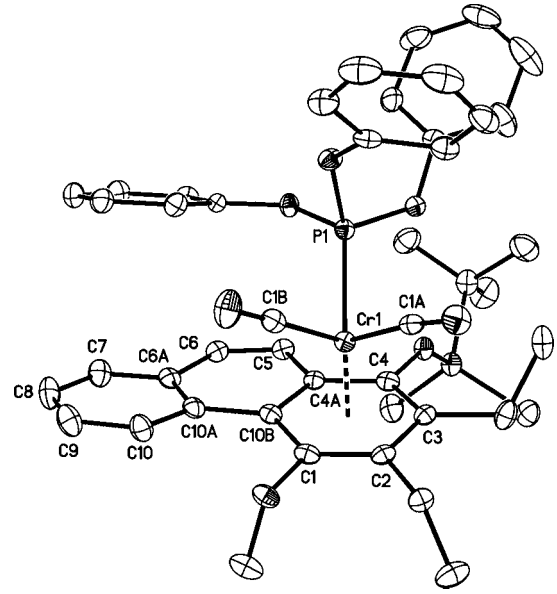

Figure 2. Molecular structure of $P(OPh)_3$ complex **4**. Hydrogen atoms have been omitted for clarity. Displacement parameters are drawn at the 50% probability level. The numbering of atoms differs from that used in the NMR characterization. Selected bond distances [Å]: Cr1−P1 2.2088(6), Cr1−C4 2.300(2), Cr1−C3 2.247(2), Cr1−C2 2.198(2), Cr1−C1 2.190(2), Cr−C10B 2.252(2), Cr1−C4A 2.309(2), Cr1-Z_{Ar} 1.740(1), Cr1−C1A 1.818(2), Cr1−C1B 1.826(2). Selected torsion angle [deg]: C10−C10A−C10B−C1 12.0(3).

above the inner bay of the phenanthrene skeleton, whereas the $P(OPh)_3$ ligand in complex **8** points toward the periphery of the arene system.[15] The Cr−P bond lengths generally range between 2.20 and 2.31 Å, with the longest distances found for the better P-donor ligands PMe_3 and PPh_3 in complexes **9** and **6/10**. The Cr−C bond lengths of the coordinated arene ring vary between 2.18 and 2.34 Å, indicating that chromium is not located above the center of the arene plane but rather shifted away from the ring junction to the π-periphery independent from the conformation of the chromium tripod. In complexes **4** and

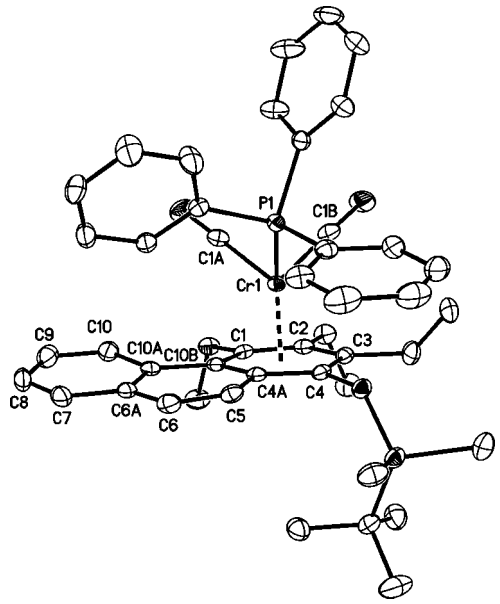

Figure 3. Molecular structure of PPh_3 complex **6**. Hydrogen atoms have been omitted for clarity. Displacement parameters are drawn at the 50% probability level. The numbering of atoms differs from that used in the NMR characterization. Selected bond distances [Å]: Cr1−P1 2.3180(5), Cr1−C4 2.3367(15), Cr1−C3 2.2690(16), Cr1−C2 2.1969(16), Cr1−C1 2.1848(16), Cr1−C10B 2.2592(15), Cr1−C4A 2.2966(15), Cr1−Z_{Ar} 1.751(1), Cr1−C1A 1.8224(18), Cr1−C1B 1.8115(17). Selected torsion angle [deg]: C10−C10A−C10B−C1 −10.4(2).

6, containing bulky phosphorus ligands, the silyl protective group adopts an *anti* conformation relative to the chromium fragment, whereas the smaller trimethylphosphite ligand prefers a *syn* conformation, as shown in complex **3**. In the rearranged $Cr(CO)_2PR_3$ complexes **7**, **9**, and **10** the phosphorus ligands point inside the phenanthrene system, while an outside orientation is observed for the $P(OPh)_3$ complex **8**. The crystallographic data for all complexes are summarized in Tables 3 and 4.

Kinetic Studies of the Coligand-Controlled Haptotropomerization. In order to elaborate the role of the P-coligand in the haptotropic metal migration, the rate constants and the activation barriers were determined by a kinetic NMR study. To secure an intramolecular course of the metal rearrangement, the reactions were performed at 75 °C in a noncoordinating solvent such as hexafluorobenzene using an external standard. Figures 8−11 show the concentration profiles for the rearrangements and the kinetic plots. The experiments reveal first-order kinetics expected for an intramolecular haptotropic metal migration in all $Cr(CO)_2PR_3$ complexes. Compared to the parent $Cr(CO)_3$ complex **1** the metal shift observed for complexes **4** and **6**, bearing the bulky and acceptor-type ligands triphenylphosphine and triphenylphosphite, is approximately 4−5 times faster, and the activation energy is decreased by ca. 5 kJ/mol (Table 5). In contrast, the smaller and better donor ligands trimethylphosphite and trimethylphosphine in complexes **3** and **5** slow down the haptotropic migration by the factor of 3 and 35 according to an increase of the free energy of activation by 3 and 10 kJ/mol, respectively.

(15) Molecular structures showing the projection of the chromium tripod onto the phenanthrene platform are depicted in the Supporting Information. For a conformational study of $Cr(CO)_3$ complexes of O-silylated phenol derivatives, see: (a) Levisalles, J.; Rose-Munch, F.; Rose, E.; Semra, A.; Garcia Oricain, J.; Jeannin, Y.; Robert, F. *J. Organomet. Chem.* **1987**, *328*, 109–122.

The rate constants and free energies of activation determined for the metal migration in the phenanthrene $Cr(CO)_2PR_3$ complexes **3**−**6** indicate that the nature of the phosphorus ligand plays a significant role in the tuning of the haptotropic migration. In order to elucidate the contribution of steric and electronic effects of the *P*-ligand, we applied the QALE method[16] for the correlation of the free energy of activation $\Delta G^{\ddagger}$ with the cone angle θ[17] and the Tolman electronic parameter χ[18] derived from the $A_{1(CO)}$ stretching frequency of $Ni(CO)_3PR_3$ complexes (Table 6, eq 1).[16]

$$\Delta G^{\ddagger} = a(\theta) + b(\chi) + c \quad [19] \qquad (1)$$

A multiple regression for the set of the four phosphorus ligands applied demonstrates that the haptotropic migration is controlled by both steric and electronic effects quantified by $a = -0.3559$ kJ mol^{-1} K^{-1}, $b = -0.5028$ kJ mol^{-1} cm^{-1}, and $c = 159.2577$ kJ mol^{-1} (Figure 12). This correlation may serve as a rationale for the experimental observation that sterically demanding ligands with considerable acceptor properties accelerate the metal migration, while small and electron-rich ligands slow it down.

Quantum Chemical Calculations on the Haptotropomerization. Density functional calculations have been performed in order to provide a more detailed insight into the course of the haptotropomerization of chromium fragments modified by *P*-coligands, in particular into the structures and relative energies of the haptotropomers and the relevant transition states. This work extends previous studies on tricarbonyl phenanthrene complexes (Scheme 4).[3]

Because of the drastically increased number of atoms resulting from the substitution of one carbon monoxide by a phosphine or phosphite coligand, most calculations were carried out for naphthalene complexes expecting that the trends for the energy barriers for the metal migration along naphthalene and phenanthrene platforms are similar.[20] The results of corresponding model calculations are compiled in Table 7. The energy barriers ΔE(**TS/S**) are given with respect to the thermodynamically less favored starting haptomer **S**. The relative energies ΔE(**NS/S**) are those of the less stable kinetic haptomer **S** with respect to the more stable regioisomer **NS** obtained from the thermoinduced metal migration.

A comparison of the barriers for the substituted (R_1 = OMe, R_2 = Et) and the unsubstituted ($R_1 = R_2$ = H) system reveals that the substitution leads to a significant decrease in the energy barriers of about 20 kJ mol^{-1} for all four ligands **L**. The energies of the transition states for the substituted naphthalene show that the highest barrier (119.7 kJ mol^{-1}) is found for L = PMe_3, which is the sterically least demanding coligand. Correspondingly the lowest energy barrier was determined for L = $P(OPh)_3$. In the calculations a clear trend of the energy barrier height due to the steric demand of the coligand is found, decreasing in the order $PMe_3 > P(OMe)_3 > PPh_3 > P(OPh)_3$ (see Figure 13). This trend is perfectly in line with the experimentally determined energy barriers. The energy barriers of the substi-

(16) (a) Giering, W. P.; Prock, A.; Wilson, M. R. *Organometallics* **2002**, *21*, 2758–2763. (b) Giering, W. P.; Prock, A.; Wilson, M. R.; Fernandez, A. L. *Organometallics* **2001**, *20*, 3429–3435. (c) Giering, W. P.; Prock, A.; Liu, H. Y.; Rahman, M. M. *Organometallics* **1987**, *6*, 650–658.

(17) (a) Tolman, C. A. *Chem. Rev.* **1977**, *77*, 313–348. (b) Bunten, K. A.; Chen, L.; Fernandez, A. L.; Poë, A. J. *Coord. Chem. Rev.* **2002**, *233−234*, 41–51.

(18) (a) Bartik, T.; Himmler, T.; Schulte, H. G.; Seevogel, K. *J. Organomet. Chem.* **1984**, *272*, 29–41. (b) Kühl, O. *Coord. Chem. Rev.* **2005**, *249*, 693–704.

(19) θ is a measure of the steric property of the ligands provided by Tolman's cone angle, while χ is the electronic parameter.

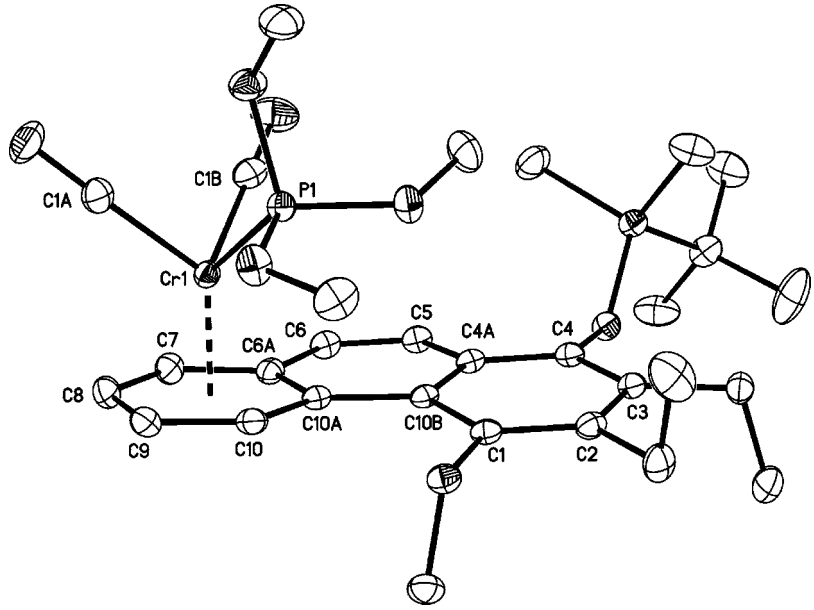

Figure 4. Molecular structure of $P(OMe)_3$ complex **7**. Hydrogen atoms have been omitted for clarity. Displacement parameters are drawn at the 50% probability level. The numbering of atoms differs from that used in the NMR characterization. Selected bond distances [Å]: Cr1−P1 2.2272(4), Cr1−C10A 2.2608(12), Cr1−C10 2.1811(13), Cr1−C9 2.2027(14), Cr1−C8 2.2004(13), Cr1−C7 2.2170(13), Cr1−C6A 2.2453(13), Cr1−Z_{Ar} 1.704(1), Cr1−C1A 1.8280(14), Cr1−C1B 1.8349(15). Selected torsion angle [deg]: C10−C10A−C10B−C1 9.6(2).

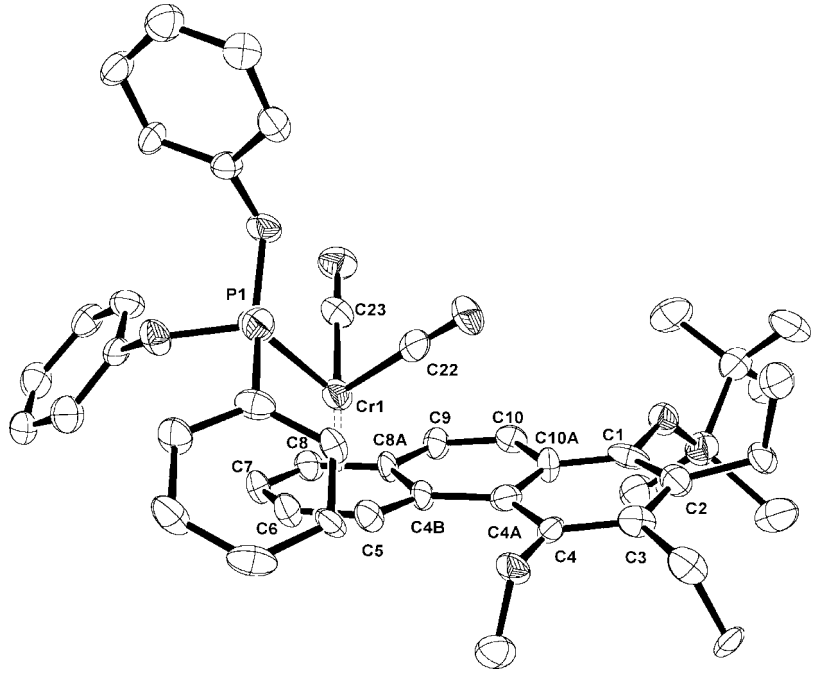

Figure 5. Molecular structure of $P(OPh)_3$ complex **8**. Hydrogen atoms have been omitted for clarity. Displacement parameters are drawn at the 50% probability level. Selected bond distances [Å]: Cr1−P1 2.204(4), Cr1−C4B 2.289(3), Cr1−C5 2.232(6), Cr1−C6 2.2179(5), Cr1−C7 2.2040(5), Cr1−C8 2.1793(3), Cr1−C8A 2.1940(4), Cr1–Z_{Ar} 1.713, Cr1−C22 1.8303(3), Cr1−C23 1.7858(5). Selected torsion angle [deg]: C4−C4A−C4B−C5 8.158(3).

tuted naphthalene complexes exhibit a nearly perfect linearity. This indicates that an increasing size of the coligand leads to a decrease of the energy barrier assisted by the electronic effect resulting from the incorporation of an oxygen functionality pointing in the same direction.

The calculated structures of naphthalene complexes bearing different phosphorus ligands are presented in Figure 14. In the transition states, the chromium adopts a trimethylenemethane-like coordination to the arene; alternating positions of the methoxy substituents relative to the chromium unit were found for the complexes bearing the sterically less demanding ligands PMe_3 and $P(OMe)_3$, while the more bulky

(20) Note that for the haptotropic migration of $Cr(CO)_3$ the transition state barriers for the unsubstituted phenanthrene (128.0 and 122.2 kJ mol^{-1}) were calculated very close to the one for naphthalene (125.9 kJ mol^{-1}): Ketrat, S.; Müller, S.; Dolg, M. *J. Phys. Chem. A* **2007**, *111*, 6094–6102.

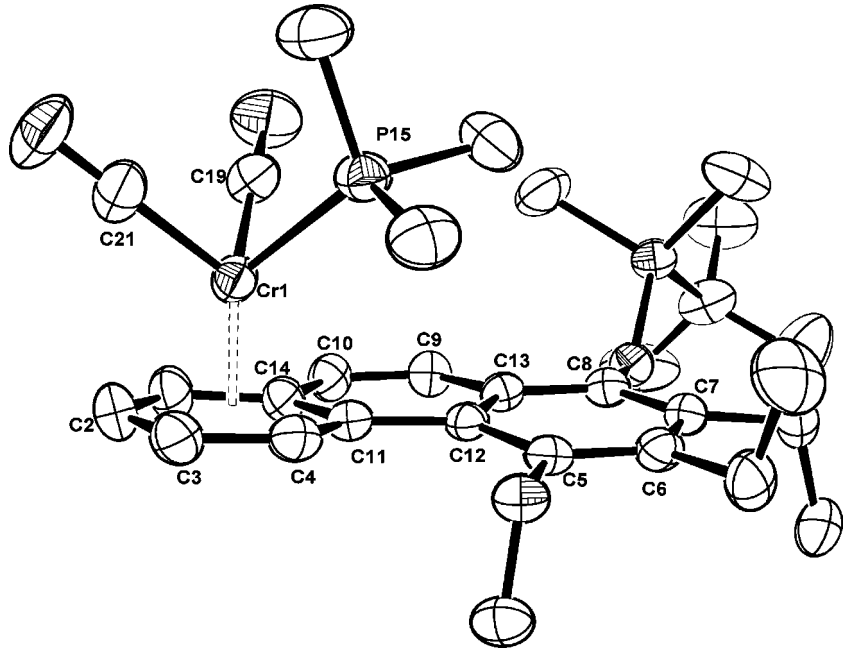

Figure 6. Molecular structure of PMe_3 complex **9**. Hydrogen atoms have been omitted for clarity. Displacement parameters are drawn at the 50% probability level. The numbering of atoms differs from that used in the NMR characterization. Selected bond distances [Å]: Cr1−P15 2.3135(9), Cr1−C1 2.181(3), Cr1−C2 2.176(3), Cr1−C3 2.204(3), Cr1−C4 2.201(3), Cr1−C11 2.269(3), Cr1−C14 2.241(3), Cr1−Z_{Ar} 1.701, Cr1−C19 1.820(3), Cr1−C21 1.822(3). Selected torsion angle [deg]: C5−C12−C11−C4 −9.3(4).

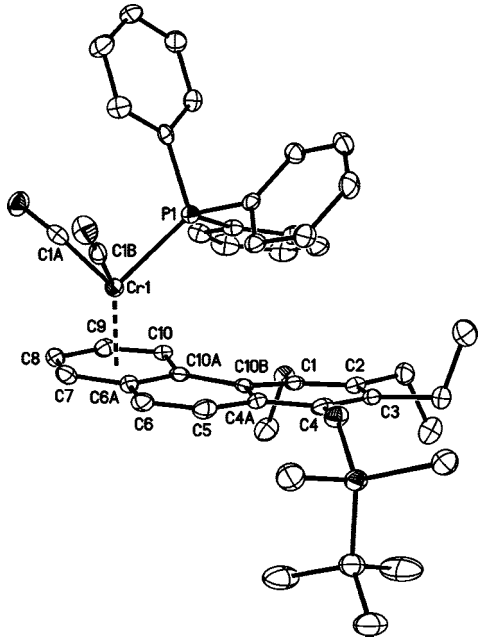

Figure 7. Molecular structure of PPh_3 complex **10**. Hydrogen atoms have been omitted for clarity. Displacement parameters are drawn at the 50% probability level. The numbering of atoms differs from that used in the NMR characterization. Selected bond distances [Å]: Cr1−P1 2.3195(8), Cr1−C7 2.183(2), Cr1−C8 2.182(2), Cr1−C9 2.216(2), Cr1−C10 2.229(2), Cr1−C10A 2.346(2), Cr1−C6A 2.277(2), Cr1−Z_{Ar} 1.736(1), Cr1−C1A 1.812(2), Cr1−C1B 1.826(2). Selected torsion angle [deg]: C10−C10A−C10B−C1 −7.5(3).

ligands PPh_3 and $P(OPh)_3$ induce a conformation bearing both methoxy groups opposite the chromium fragment.

In order to confirm that the naphthalene system is an adequate model to describe the experimental findings, we calculated all relevant structures for the two phenanthrene complexes bearing the *P*-coligands $P(OMe)_3$ and PPh_3, which count 65 and 83 atoms, respectively. The relative energies, using the same conventions as for Table 6, are listed in Table 8.

The values presented in Table 8 show that compared to naphthalene complexes the situation is more complicated in phenanthrene compounds due to the increased number of transition states. Nevertheless, it can be stated that the energy barriers are in the range of the experimental values and decrease significantly when the bulk of the migrating group

Table 3. Crystallographic Data for Complexes 3, 4, and 6

	3	**4**	**6**
empirical formula	$C_{30}H_{43}CrO_7PSi$	$C_{45}H_{49}CrO_7PSi$	$C_{45}H_{49}CrO_4PSi$
M [g/mol]	626.70	812.90	764.90
T [K]	123(2)	123(2)	123(2)
λ [Å]	Mo Kα 0.71073	Mo Kα 0.71073	Mo Kα 0.71073
cryst syst	monoclinic	triclinic	triclinic
space group	$P2_1/c$ (no. 14)	$P\bar{1}$ (no. 2)	$P\bar{1}$ (no. 2)
a [Å]	15.4755(4)	9.3080(1)	9.4311(1)
b [Å]	9.4598(3)	11.1984(2)	11.9278(1)
c [Å]	21.3731(6)	21.5305(5)	19.7424(3)
α [deg]	90	80.901(1)	73.265(1)
β [deg]	98.010(2)	84.642(1)	83.572(1)
γ [deg]	90	65.482(1)	68.017(1)
V [Å^3]	3098.39(15)	2015.21(6)	1972.16(4)
Z	4	2	2
cryst size [mm]	0.40 × 0.25 × 0.10	0.30 × 0.15 × 0.05	0.35 × 0.10 × 0.05
ρ(calcd) [g/cm]	1.343	1.340	1.288
μ [mm^{-1}]	0.503	0.404	0.403
F(000)	1328	856	808
θ range [deg]	3.29 to 25.03	2.96 to 25.03	3.17 to 27.47
index ranges	$-18 \le h \le 13$ $-10 \le k \le 11$ $-25 \le l \le 24$	$-11 \le h \le 11$ $-13 \le k \le 13$ $-25 \le l \le 25$	$-12 \le h \le 12$ $-15 \le k \le 15$ $-25 \le l \le 25$
total reflns	11 831	17 177	32 884
unique reflns	5059	7042	8873
R(int)	0.0304	0.0326	0.0388
R for ($I > 2\sigma(I)$)	0.0380	0.0339	0.0347
wR^2 (all data)	0.0904	0.0845	0.0911
goodness of fit on F^2	1.037	0.994	1.050
largest diff peak and hole [e Å^{-3}]	0.324/−0.354	0.307/−0.312	0.341/−0.383

Table 4. Crystallographic Data for Phenanthrene Complexes 7−10

	7	8	9	10
empirical formula	$C_{30}H_{43}CrO_7PSi$	$C_{45}H_{49}CrO_7PSi$	$C_{30}H_{43}CrO_4PSi$	$C_{45}H_{49}CrO_4PSi$
M [g/mol]	626.70	812.90	578.70	764.90
T [K]	123(2)	123(2)	223(2)	123(2)
λ [Å]	Mo Kα 0.71073	Mo Kα 0.71073	Mo Kα 0.71073	Mo Kα 0.71073
cryst syst	monoclinic	monoclinic	monoclinic	triclinic
space group	$P2_1/c$ (no. 14)	$P2_1/c$ (no. 14)	$P2_1/c$ (no. 14)	$P\bar{1}$ (no. 2)
a [Å]	14.3749(1)	26.672(5)	14.813(1)	8.9334(3)
b [Å]	17.3537(1)	11.080(2)	17.070(1)	14.0088(5)
c [Å]	13.2375(1)	14.165(5)	13.084(1)	17.0355(8)
α [deg]	90	90	90	88.580(2)
β [deg]	108.132(1)	98.120(9)	108.11(1)	75.167(2)
γ [deg]	90	90	90	73.085(2)
V [Å^3]	3138.21(4)	4144.2(18)	3144.5(4)	1968.88(13)
Z	4	4	4	2
cryst size [mm]	0.40 × 0.20 × 0.10	0.16 × 0.08 × 0.04	0.40 × 0.30 × 0.20	0.30 × 0.10 × 0.05
ρ(calcd) [g/cm]	1.326	1.303	1.222	1.290
μ [mm^{-1}]	0.497	0.393	0.484	0.404
F(000)	1328	1712	1232	808
θ range [deg]	2.98 to 27.48	2.40 to 25.00	1.87 to 30.42	2.98 to 25.03
index ranges	$-18 \le h \le 18$	$-28 \le h \le 31$	$-21 \le h \le 20$	$-10 \le h \le 10$
	$-22 \le k \le 22$	$-12 \le k \le 13$	$-23 \le k \le 23$	$-16 \le k \le 16$
	$-17 \le l \le 17$	$-15 \le l \le 15$	$-18 \le l \le 18$	$-18 \le l \le 20$
total reflns	64 161	16 905	21 961	16 563
unique reflns	7165	6279	9291	6924
R(int)	0.0390	0.2538	0.066	0.0434
R for ($I > 2\sigma(I)$)	0.0277	0.1050	0.0622	0.0368
wR^2 (all data)	0.0793	0.2803	0.1791	0.0756
goodness of fit on F^2	1.051	0.935	0.998	0.903
largest diff peak and hole [e Å^{-3}]	0.328/−0.385	0.391/−0.276	0.406/−0.804	0.311/−0.420

increases, confirming that the use of the model system naphthalene produces reliable results. The calculation of the minimum structure of the middle ring complex **M** resulted in a rather small energy difference between complexes **M** and **S**, especially for L = PPh_3. This may be a reason for the acceleration of the migration for the bulkier metal fragments as found in the experiments.

In order to evaluate the quality of the theoretical approach, a comparison of selected bond lengths is presented in Table 9 for L = PPh_3. In general, there is a very good agreement of the calculated and the experimentally obtained structure with maximum deviations of about 0.05 Å. The orientation of the methoxy and ethyl substituents is identical in the calculations and the X-ray structure; that is, both methoxy groups and one ethyl group of the substituted ring point to the opposite side of the coordinated chromium fragment. We note that other orientations of these substituents might lead to local minima that are several kJ/mol higher in energy.

Conclusion

A study of the haptotropic metal migration in $Cr(CO)_2PR_3$ complexes of phenanthrene demonstrated that the exchange of a carbonyl ligand of $Cr(CO)_3$-phenanthrene complexes for a phosphorus ligand can be applied to tune the metal shift depending on the steric and electronic effects of the coligand. The $Cr(CO)_2PR_3$ (R = OMe, Me, Ph, OPh) complexes were prepared via photoinduced ligand substitution of $Cr(CO)_3$-phenanthrene complexes in tetrahydrofuran. A kinetic analysis of the haptotropic metal migration via NMR spectroscopy in hexafluorobenzene reveals that the migration is first order. The contribution of steric and electronic ligand effects to the metal isomerization has been investigated using the QALE method. Bulky ligands such as $P(OPh)_3$ or PPh_3 accelerate the metal isomerization, and small or electron-rich ligands such as $P(OMe)_3$ or PMe_3 slow it down. The DFT calculations support the experimental work. The results for a smaller

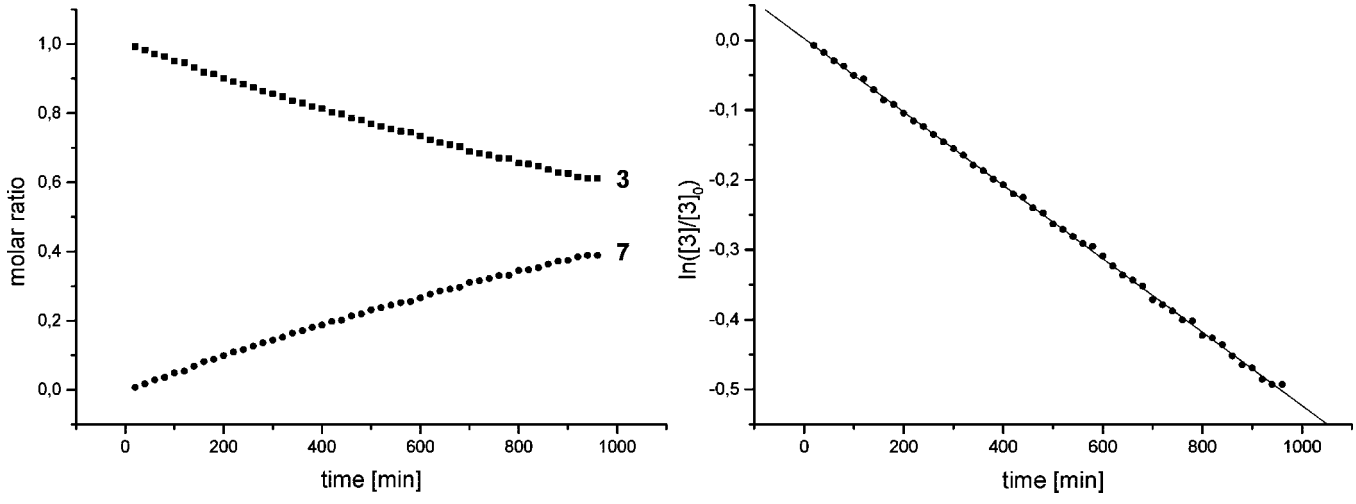

Figure 8. Concentration profile and kinetic plot for the rearrangement of the trimethylphosphite complex **3**.

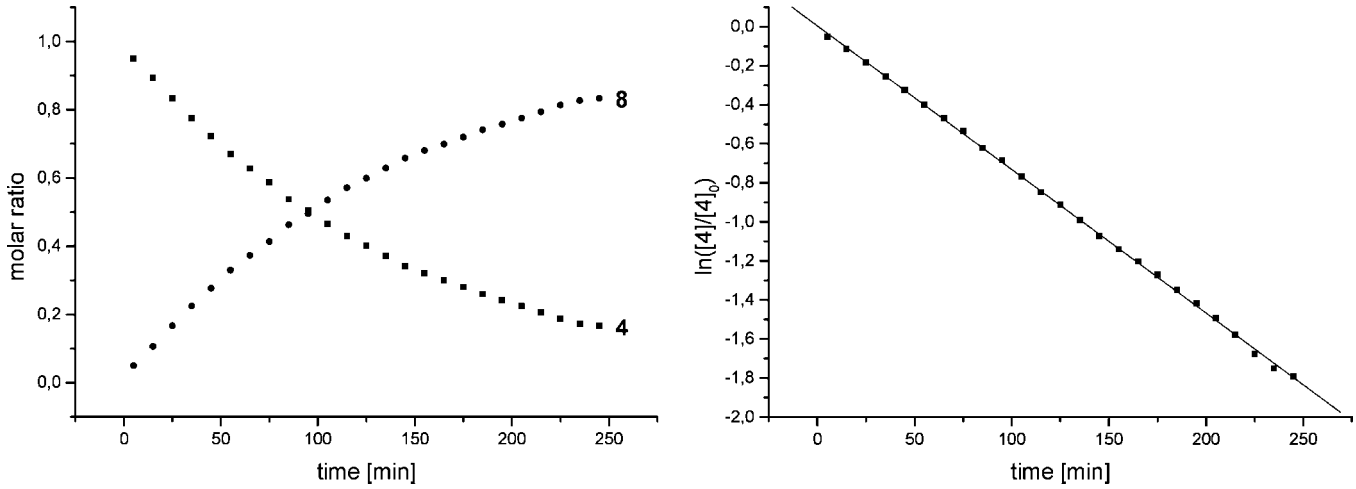

Figure 9. Concentration profile and kinetic plot for the rearrangement of the triphenylphosphite complex **4**.

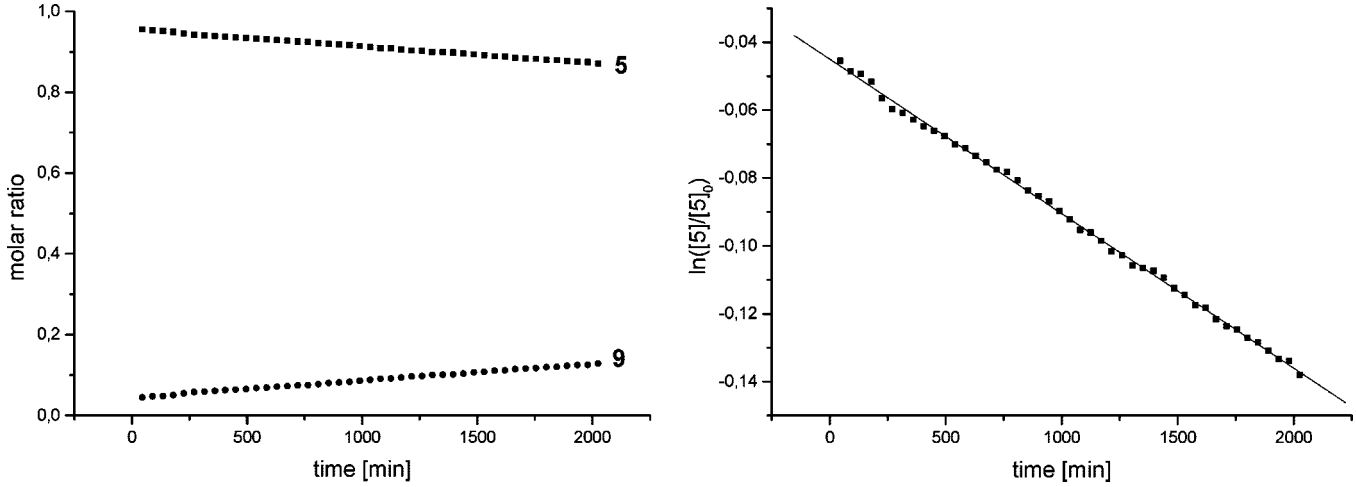

Figure 10. Concentration profile and kinetic plot for the rearrangement of the trimethylphosphine complex **5**.

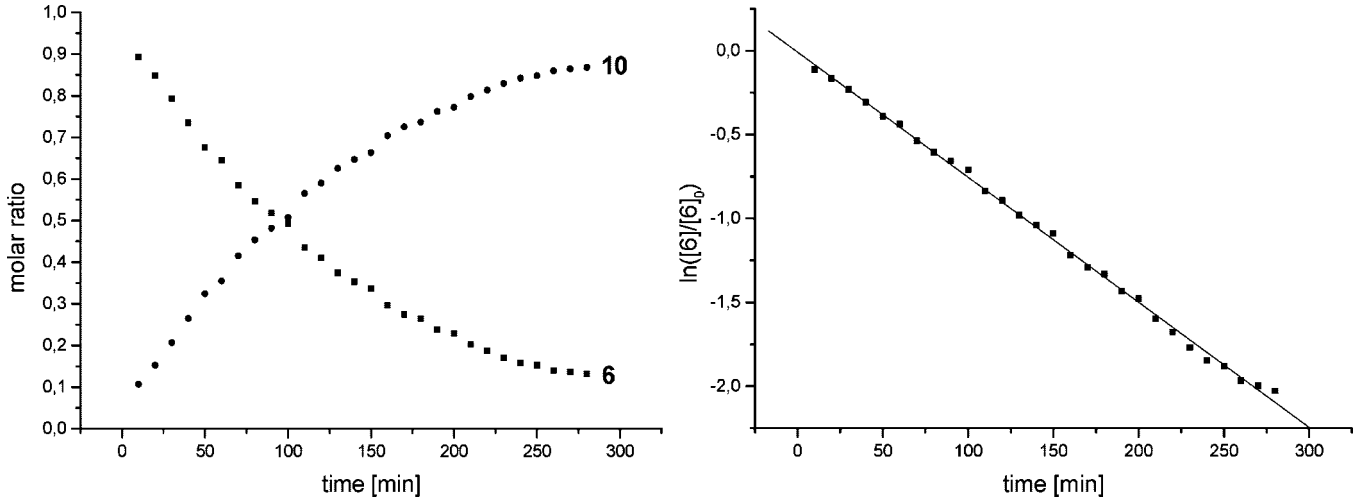

Figure 11. Concentration profile and kinetic plot for the rearrangement of the triphenylphosphine complex **6**.

model system (naphthalene instead of phenanthrene) exhibit a clear linearity of the energy barriers with respect to the size of the coligand.

Experimental Section

General Procedures. All reactions were carried out under an argon atmosphere using conventional Schlenk techniques. Dichloromethane was dried by distillation from calcium hydride, petroleum ether by distillation from lithium aluminum hydride, and tetrahydrofuran and di-*n*-butyl ether by distillation from sodium. Deuterated solvents and hexafluorobenzene were saturated with argon using three cycles of freeze, pump, and thaw before use. $P(OMe)_3$, $P(OPh)_3$, PPh_3, and PMe_3 (1 M solution in THF) were used as received from Fluka. Macherey Nagel silica gel 60 (0.015−0.025 mm) was used for column chroma-

Table 5. Rate Constants and Activation Barriers (with standard deviations) of the Haptotropic Migration in Complexes 3−6

$Cr(CO)_2L$	T [K][a]	k [s^{-1}]	$\Delta G^{\ddagger}$ [kJ mol^{-1}]
L= $P(OMe)_3$	348	(5.26±0.2) × 10−4	107.5 ± 0.3
L = $P(OPh)_3$	348	(7.36±0.3) × 10−3	99.89 ± 0.3
L = PPh_3	348	(7.46±0.5) × 10−3	99.85 ± 0.3
L = PMe_3	348	(4.55±0.3) × 10−5	114.3 ± 0.3
L = CO[b]	348	(1.6±0.2) × 10−3	104.3 ± 0.3

[a] T = 348 K measured in C_6F_6. [b] Ref 3.

Table 6. Free Energy of Activation of the Haptotropomerization of Complexes 3−6, Cone Angles, and Electronic Parameters for the PR_3 Ligands Applied

PR_3	$\Delta G^{\ddagger}$ [kJ mol^{-1}]	θ [deg][a]	χ [cm^{-1}][b]
$P(OMe)_3$	107.5 ± 0.3	107	24.10
$P(OPh)_3$	99.89 ± 0.3	128	30.20
PPh_3	99.85 ± 0.3	145	13.25
PMe_3	114.3 ± 0.3	118	8.55

[a] Cone angles taken from ref 17. [b] Electronic parameters taken from ref 18a.

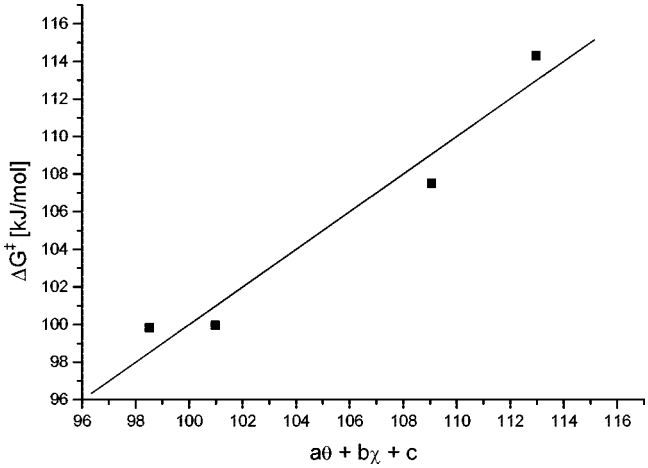

Figure 12. QALE correlation: Fit of experimental $\Delta G^{\ddagger}$ values vs $a(\theta) + b(\chi) + c$.

Scheme 4. Schematic Representation of the Calculated Naphthalene and Phenanthrene Complexes

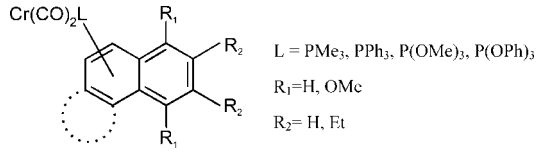

tography. Infrared spectra were recorded on a Nicolet Magna 550. NMR spectra were measured on Bruker DRX-300, -400, and -500 spectrometers at room temperature. Mass spectra (EI-MS) were recorded on a Kratos MS 50.

General Procedure for the Synthesis of $Cr(CO)_2PR_3$ Phenanthrene Complexes. 1 mmol of complex **1** or **2** was dissolved in 50 mL of THF and irradiated 3 h with a HPK 125 medium-pressure mercury lamp at −40 °C. The phosphite or phosphine was added as a solution in tetrahydrofuran, and the reaction mixture was allowed to warm to room temperature and stirred for 2 h. All volatile components were removed, and the residue was subjected to column chromatography.

Dicarbonyl(trimethylphosphite)[(η^6-1,2,3,4,4A,10A)-1-*tert*-butyldimethylsilyloxy-2,3-diethyl-4-methoxyphenanthrene]chromium (3). Yield: 420 mg (67%). R_f = 0.5 (CH_2Cl_2). Yield: 420 mg (67%). R_f = 0.5 (CH_2Cl_2). IR (PE): $\nu_{(C=O)}$ 1897 (vs, A_1), 1888 (vs, A_1), 1849 (m), 1839 (s, B_1) cm^{-1}. ^{1}H NMR (400 MHz, $CDCl_3$): δ 9.18 (d, $^3J_{HH}$ = 8.5 Hz, 1H, H5), 7.71 (d, $^3J_{HH}$ = 9.3 Hz, 1H, H9/10), 7.68 (d, $^3J_{HH}$ = 7.7 Hz, 1H, H8), 7.59 (m, 1H, H6/7), 7.53 (m, 1H, H6/7), 7.42 (d, $^3J_{HH}$ = 9.3 Hz, 1H, H9/10), 3.75 (s, 3H, OCH_3), 3.08 (d, $^2J_{HP}$ = 11.2 Hz, 9H, $P(OMe_3)_3$), 2.85−2.65 (m, 4H, CH_2), 1.44 (t, $^3J_{HH}$ = 7.52 Hz, 3H, CH_3), 1.39 (t, $^3J_{HH}$ = 7.52 Hz, 3H, CH_3), 1.11 (s, 9H, $C(CH_3)_3$), 0.42 (s, 3H, $SiCH_3$), 0.36 (s, 3H, $SiCH_3$) ppm. ^{13}C NMR (100 MHz, $CDCl_3$): δ 239.0 (d, $^2J_{CP}$ = 33.9 Hz, Cr(CO)), 238.3 (d, $^2J_{CP}$ = 33.1, Cr(CO)), 132.7, 131.2 (2C, C1/4), 130.2, 129.0 (ArC), 128.6, 127.9 (ArCH), 127.2 (d, $^3J_{HP}$ = 4 Hz, ArCH), 126.9, 123.3 (ArCH), 105.1, 100.6, 93.2, 92.9 (ArC), 62.7 (OCH_3), 50.1 (d, $^3J_{CP}$ = 2 Hz, $P(OCH_3)_3$), 26.3 ($C(CH_3)_3$), 21.5, 20.9 (CH_2), 19.1 ($C(CH_3)_3$), 16.3, 16.0 (CH_3), −1.9 ($SiCH_3$), −2.6 ($SiCH_3$) ppm. ^{31}P NMR (202 MHz, $CDCl_3$): δ 215.1 ppm. MS (EI): m/z (%) = 626 (68) [M^+], 595 (22) [M^+ − OMe], 570 (20) [M^+ − 2CO], 446 (30) [M^+ − 2CO − $P(OMe)_3$], 394 (100) [M^+ − $Cr(CO)_2P(OMe)_3$], 379 (30) [M^+ − $Cr(CO)_2P(OMe)_3$ − Me], 176 (8) [$Cr(CO)_2P(OMe)_3^+$], 73 (30) [$SiMe_3^+$]. HR-MS: calcd for $C_{30}H_{43}CrO_7PSi$ 626.19208, found 626.19160.

Table 7. Calculated Energy Barriers and Relative Energies of the Naphthalene Complexes Depicted in Scheme 4[a]

		R_1 = OMe, R_2 = Et			$R_1 = R_2$ = H
L	$\Delta G^{\ddagger}$ exptl	ΔE (**TS/S**)	difference calc/exptl	ΔE (**NS/S**[b])	ΔE(**TS/S**)
PMe_3	114.3	119.7	5.4	−23.0	137.7
$P(OMe)_3$	107.5	114.3	6.8	−15.5	132.6
PPh_3	99.85	110.5	10.7	−25.5	133.5
$P(OPh)_3$	99.89	104.2	4.3	−25.5	128.0
CO	104.3	106.3	2.0	−11.3	122.2

[a] A single-point calculation with the solvent model COSMO has been performed for all structures. Experimentally determined free energies of activation $\Delta G^{\ddagger}$ for the related phenanthrene systems from Table 5 are given for comparison. All energies are listed in kJ mol^{-1}. [b] **NS**: $Cr(CO)_2L$ is coordinated to the nonsubstituted ring, **S**: $Cr(CO)_2L$ is coordinated to the hydroquinoid ring.

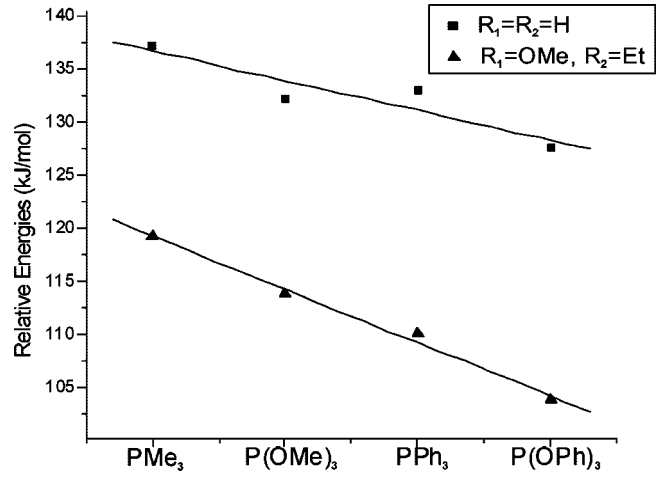

Figure 13. Relative energies of the transition states of all four phosphorus ligands for substituted (▲) and unsubstituted (■) naphthalene.

Dicarbonyl(triphenylphosphite)[(η^6-1,2,3,4,4A,10A)-1-*tert*-butyldimethylsilyloxy-2,3-diethyl-4-methoxyphenanthrene]chromium (4). Yield: 436 mg (57%). R_f = 0.4 (2:1 petroleum ether/CH_2Cl_2). IR (PE): $\nu_{(C=O)}$ 1903 (vs, A_1), 1853 (s, B_1) cm^{-1}. ^{1}H NMR (400 MHz, $CDCl_3$): δ 9.16 (dd, $^3J_{HH}$ = 7.2 Hz, $^4J_{HH}$ = 1.9 Hz, 1H, H5), 7.63−7.51 (m, 4H), 7.16−7.06 (m, 7H), 6.83−6.77 (m, 6H), 3.80 (s, 3H, OCH_3), 2.92 (m, 2H, CH_2), 2.65 (m, 2H, CH_2), 1.40 (t, $^3J_{HH}$ = 7.5 Hz), 1.32 (t, $^3J_{HH}$ = 7.5 Hz), 1.05 (s, 9H, $C(CH_3)_3$), 0.35 (s, 3H, $SiCH_3$), 0.28 (s, 3H, $SiCH_3$). ^{13}C NMR (100 MHz, $CDCl_3$): δ 238.2 (d, $^2J_{CP}$ = 30.7 Hz, Cr(CO)), 237.7 (d, $^2J_{CP}$ = 31.2 Hz, Cr(CO)), 152.2 (d, $^2J_{CP}$ = 10.1 Hz, POC), 133.4 (C1/C4), 131.7 (C1/C4), 130.8 (C_{Aryl}), 129.6 (C_{Aryl}), 128.8 (POC-CH_{Aryl}), 128.3, 127.6, 127.3, 126.7, 123.6 (5C, CH_{Aryl}), 123.2 (POC-CH_{Aryl}),

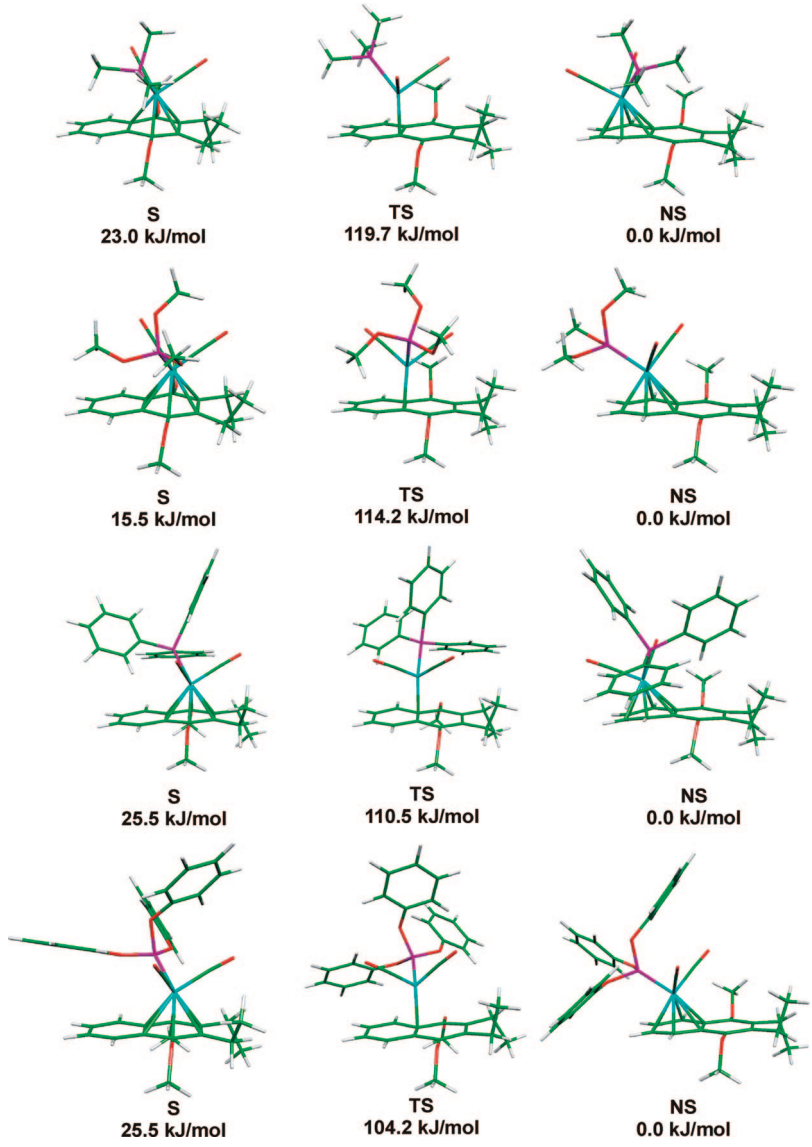

Figure 14. Calculated structures for 1,4-dimethoxy-2,3-diethylnaphthalene $Cr(CO)_2PR_3$ complexes.

Table 8. Relative Energies of the Transition States for the Migration of the $Cr(CO)_2L$ Fragment on the Phenanthrene Platform

L[a]	$P(OMe)_3$	PPh_3	
$\Delta G^{\neq}$ exp.	107.5	99.9	
ΔE (TSIa/S)	116.3	-[b]	
ΔE (TSIIa/S)	120.9	104.1	
ΔE (TSIb/S)	107.1	94.2	
ΔE (TSIIb/S)	113.8	107.9	
ΔE (NS/S)	-26.8	-33.6	
ΔE (M/S)[c]	25.6	17.4	

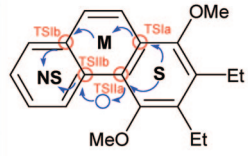

[a] All values in kJ mol^{-1}. [b] Transition state could not be found. [c] **M**: $Cr(CO)_2L$ is coordinated to the middle ring.

Table 9. Comparison of Selected Bond Lengths of the 1,4-Dimethyl-2,3-diethylphenanthrene-$Cr(CO)_2PPh_3$ Complex (bond lengths in Å)

Parameter	Exp.	Calc.	
Cr1-P1	2.318	2.369	-0.051
Cr1-C1	2.184	2.207	-0.023
Cr1-C2	2.196	2.213	-0.017
Cr1-C3	2.269	2.259	0.010
Cr1-C4	2.337	2.283	0.054
Cr1-C4a	2.296	2.336	-0.04
Cr1-C10b	2.259	2.309	-0.05
Cr1-C1a	1.822	1.826	-0.004
Cr1-C1b	1.811	1.810	0.001

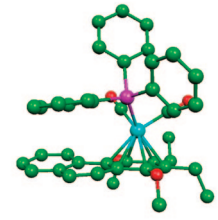

121.7 (CH_{Aryl}), 121.0 (POC-CH_{Aryl}), 107.6, 100.9, 96.4, 92.3 (C2, C3, C4a, C10a), 63.7 (OCH_3), 26.3 (3C, $C(CH_3)_3$), 21.3, 20.6 (CH_2), 19.1 ($C(CH_3)_3$, 16.3, 15.6 (CH_3), −2.3, −2.5 ($SiCH_3$). ^{31}P NMR (202 MHz, $CDCl_3$): δ 189.9. MS (EI): *m/z* (%) 812 (7) [M^+], 756 (18) [$M^+ - 2CO$], 539 (5) [$M^+ - 2CO - P(OPh)_2$], 446 (5) [$M^+ - 2CO - P(OPh)_3$], 394 (100) [$M^+ - Cr(CO)_2P(OPh)_3$], 362 (45)

(21) Ahlrichs, R.; et al. *Turbomole 5, Institut für Physikalische Chemie*; Universität Karlsruhe, 2002.

$[Cr(CO)_2P(OPh)_3^+]$, 310 (22) $[P(OPh)_3^+]$, 217 (65) $[P(OPh)_2^+]$. HR-MS: calcd for $C_{45}H_{49}CrO_7PSi$ 812.23903, found 812.23944.

Dicarbonyl(trimethylphosphine)[(η^6-1,2,3,4,4A,10A)-1-*tert*-butyldimethylsilyloxy-2,3-diethyl-4-methoxyphenanthrene]chromium (5). Yield: 220 mg (38%). R_f = 0.4 (1:1 petroleum ether/CH_2Cl_2). IR (PE): $\nu_{(C=O)}$ 1878 (vs, A_1), 1830 (s, B_1) cm^{-1}. ^1H NMR (500 MHz, CD_2Cl_2): δ 9.16 (d, $^3J_{HH}$ = 8.3 Hz, 1H, H5), 7.68 (dd, $^3J_{HH}$ = 7.6 Hz, $^4J_{HH}$ = 1.6 Hz, 1H, H8), 7.63 (d, $^3J_{HH}$ = 9.3 Hz, 1H, H9/10), 7.66−7.57 (m, 2H, H6/7), 7.24 (d, $^3J_{HH}$ = 9.3 Hz, 1H, H9/10), 3.82 (s, 3H, OCH_3), 3.02−2.9 (m, 1H, CH_2), 2.8−2.63 (m, 3H, CH_2), 1.42 (t, $^3J_{HH}$ = 7.5 Hz, 3H, CH_2CH_3), 1.40 (t, $^3J_{HH}$ = 7.5 Hz, 3H, CH_2CH_3), 1.11 (s, 9H, $C(CH_3)_3$), 0.95 (d, $^3J_{PH}$ = 7.8 Hz, 9H, $P(CH_3)_3$), 0.37 (s, 3H, $SiCH_3$), 0.34 (s, 3H, $SiCH_3$) ppm. ^{13}C NMR (125 MHz, CD_2Cl_2): δ 239.6 (d, $^1J_{CP}$ = 21.1 Hz, Cr(CO)), 238.9 (d, $^1J_{CP}$ = 21.1 Hz, Cr(CO)), 132.5 (C1/4), 130 (C1/4), 129.4, 129.2 (2C, C4b/8a), 127.8, 127.6, 126.7, 126.5, 124.5, 123.9 (6C, ArCH), 102.4, 99.5, 93.8, 90.9 (4C, C4a, C10a, C3, C2), 62.9 (OCH_3), 25.7 (C(*C*H_3)$_3$), 21.2, 20.2 ($2CH_2$), 18.6 (d, $^1J_{CP}$ = 22.5 Hz, $P(CH_3)_3$), 18.5 (*C*$(CH_3)_3$), 16.4, 15.4 ($2CH_2$*C*H_3), −3.2 (2 $Si(CH_3)$) ppm. ^{31}P NMR (202 MHz, CD_2Cl_2): δ 35.0 ppm. MS (EI): *m*/*z* (%) 578 (1) $[M^+]$, 522 (15) $[M^+ - 2CO]$, 446 (4) $[M^+ - 2CO - PMe_3]$, 394 (100) $[M^+ - Cr(CO)_2PMe_3]$, 379 (39) $[M^+ - Cr(CO)_2PMe_3 - CH_3]$. HR-MS: calcd for $C_{30}H_{43}CrO_4PSi$ 578.2073, found 578.2075.

Dicarbonyl(triphenylphosphine)[(η^6-1,2,3,4,4A,10A)-1-*tert*-butyldimethylsilyloxy-2,3-diethyl-4-methoxyphenanthrene]chromium (6). Yield: 458 mg (60%). R_f = 0.6 (2:1 petroleum ether/CH_2Cl_2). IR (PE): $\nu_{(C=O)}$ 1891 (vs, A_1), 1886 (s), 1843 (s, B_1), 1835 (s, B_1) cm^{-1}. ^1H NMR (300 MHz, $CDCl_3$): δ 9.08 (d, $^3J_{HH}$ = 8.1 Hz, 1H, H5), 7.66 (dd, $^3J_{HH}$ = 7.6 Hz, $^4J_{HH}$ = 1.7 Hz, 1H, H6/8), 7.59 (d, $^3J_{HH}$ = 9.3 Hz, 1H, H9/10), 7.57−7.44 (m, 7H), 7.37 (d, $^3J_{HH}$ = 9.3 Hz, 1H, H9/10), 7.33−7.20 (m, 9H), 3.71 (s, 3H, OCH_3), 2.90−2.50 (m, 4H, $2CH_2CH_3$), 1.29 (t, $^3J_{HH}$ = 7.45 Hz, 3H, CH_3), 1.28 (t, $^3J_{HH}$ = 7.5 Hz, 3H, CH_3), 1.04 (s, 9H, $C(CH_3)_3$), 0.29 (s, 3H, $SiCH_3$), 0.28 (s, 3H, $SiCH_3$) ppm. ^{13}C NMR (125 MHz, $CDCl_3$): δ 242.9 (d, $^2J_{CP}$ = 19.7 Hz, Cr(CO)), 242.5 (d, $^2J_{CP}$ = 19.2 Hz, Cr(CO)), 137.9 (d, $^1J_{CP}$ = 32 Hz, 3PC), 133.6 (d, $^2J_{CP}$ = 10.6 Hz, 6PC*C*H), 132.6 (C1/4), 130.1, 129.7 (2C, C4b/8a), 128.6 (C1/4), 128.4, 128.3, 128.2 (3C, Ar*C*H), 128.1 (3 PCCH-CH*C*H), 127.7 (Ar*C*H), 127.1 (d, $^3J_{CP}$ = 8.6 Hz, 6PCCH*C*HCH), 126.4, 122.6 (2C, Ar*C*H), 102.5, 99.5, 94.4, 92.9 (4C, C2, C3, C4a, C10a), 61.9 (OCH_3), 26.5 (C(*C*H_3)$_3$), 21.4, 21.3 (2C, *C*H_2CH_3), 19.3 (*C*$(CH_3)_3$), 16.1, 15.9 (2C, CH_2CH_3), −1.9, −2.5 (2C, $SiCH_3$) ppm. ^{31}P NMR (202 MHz, $CDCl_3$): δ 88.9 ppm. MS (EI): *m*/*z* (%) 762 (40) $[M^+]$, 708 (60) $[M^+ - 2CO]$, 446 (8) $[M^+ - 2CO - PPh_3]$, 394 (100) $[M^+ - Cr(CO)_2PPh_3]$, 379 (30) $[M^+ - Cr(CO)_2PPh_3 - CH_3]$, 262 (90) $[PPh_3^+]$. HR-MS: calcd for $C_{45}H_{49}CrO_4PSi$ 764.25429, found 764.25282.

Dicarbonyl(trimethylphosphite)[(η^6-4B,5,6,7,8,8A)-1-*tert*-butyldimethylsilyloxy-2,3-diethyl-4-methoxyphenanthrene]chromium (7). Yield: 470 mg (75%). R_f = 0.5 (CH_2Cl_2). IR (PE): $\nu_{(C=O)}$ 1907 (vs, A_1), 1859 (s, B_1) cm^{-1}. ^1H NMR (400 MHz, $CDCl_3$): δ 7.70 (d, $^3J_{HH}$ = 9.4 Hz, 1H, H9/10), 7.50 (ddd, $^3J_{HH}$ = 6.9 Hz, $^3J_{HP}$ = 3.8 Hz, $^4J_{HH}$ = 0.9 Hz 1H, H5), 7.13 (d, $^3J_{HH}$ = 9.4 Hz, 1H, H9/10), 5.62 (d, $^3J_{HH}$ = 6.3 Hz, 1H, H8), 5.28 (m, 1H, H6/7), 5.19 (m, 1H, H6/7), 3.79 (s, 3H, OCH_3), 3.28 (d, $^3J_{HP}$ = 11.3 Hz, 9H, $P(OMe)_3$), 2.93−2.71 (m, 4H, $2CH_2$), 1.28 (t, $^3J_{HH}$ = 7.44 Hz, 3H, CH_3), 1.14 (t, $^3J_{HH}$ = 7.44 Hz, 3H, CH_3), 1.08 (s, 9H, $C(CH_3)_3$), 0.16 (s, 3H, $SiCH_3$), 0.14 (s, 3H, $SiCH_3$) ppm. ^{13}C NMR (100 MHz, $CDCl_3$): δ 237.9 (d, $^2J_{CP}$ = 32.9 Hz, Cr(CO)), 237.2 (d, $^2J_{CP}$ = 31.7 Hz, Cr(CO)), 151.7 (ArC, C1/4), 146.1 (ArC, C1/4), 136.9 (ArCH), 133.4 (ArCH), 125.6 (ArCH), 125.0 (ArC), 123.7 (ArC), 100.6 (d, $^3J_{CP}$ = 1.2 Hz, ArC), 100.3 (ArC), 90.1, 88.7, 88.0, 87.6 (4C, ArC), 61.3 (OCH_3), 50.7 (d, $^3J_{CP}$ = 3 Hz, $P(OMe)_3$), 26.1 (C(*C*H_3)$_3$), 20.7, 20.3 (CH_2), 18.7 (*C*$(CH_3)_3$), 15.9, 14.8 (CH_3), −3.2, −3.3 ($SiCH_3$) ppm. ^{31}P NMR (202 MHz, $CDCl_3$): δ 219.8 ppm. MS (EI): *m*/*z* (%) 626 (20) $[M^+]$, 595 (10) $[M^+ - OMe]$, 570 (100) $[M^+ - 2CO]$, 446 (65) $[M^+ - 2CO - P(OMe)_3]$, 394 (60) $[M^+ - Cr(CO)_2P(OMe)_3]$, 379 (15) $[M^+ - Cr(CO)_2P(OMe)_3 - Me]$, 293 (20) $[M^+ - Cr(CO)_2P(OMe)_3 - Me - {}^tBu]$, 265 (5) $[M^+ - Cr(CO)_2P(OMe)_3 - Me - {}^tBu - Et]$, 176 (10) $[Cr(CO)_2P(OMe)_3^+]$, 73 (30) $[SiMe_3^+]$. HR-MS: calcd for $C_{30}H_{43}CrO_7PSi$ 626.19208, found 626.1928.

Dicarbonyl(triphenylphosphite)[(η^6-4B,5,6,7,8,8A)-1-*tert*-butyldimethylsilyloxy-2,3-diethyl-4-methoxyphenanthrene]chromium (8). Yield: 520 mg (64%). R_f = 0.3 (2:1 petroleum ether/CH_2Cl_2). IR (PE): $\nu_{(C=O)}$ 1922 (vs, A_1), 1870 (s, B_1) cm^{-1}. ^1H NMR (300 MHz, $CDCl_3$): δ 7.51 (d, $^3J_{HH}$ = 9.2 Hz, 1H, H9/10), 7.22−6.95 (m, 16H), 6.60 (d, $^3J_{HH}$ = 9.2 Hz, 1H, H9/10), 4.95 (d, 6.4 Hz, 1H, H8), 4.63 (m, 1H, H6/7), 4.41 (m, 1H, H6/7), 3.60 (s, 3H, OCH_3), 2.77−2.55 (m, 4H, CH_2), 1.12 (t, $^3J_{HH}$ = 7.3 Hz, 3H, CH_3), 1.01 (t, $^3J_{HH}$ = 7.4 Hz, 3H, CH_3), 0.96 (s, 9H, $C(CH_3)_3$), 0.02 (s, 3H, $SiCH_3$), −0.01 (s, 3H, $SiCH_3$). ^{13}C NMR (75 MHz, $CDCl_3$): δ 236.1 (d, $^2J_{CP}$ = 32.3 Hz, Cr(CO)), 235.9 (d, $^2J_{CP}$ = 32.9 Hz, Cr(CO)), 152.4 (d, $^2J_{CP}$ = 7.2 Hz, POC), 151.5, 146.3 (C1/4), 137.2, 133.8 (C_{Aryl}), 129.3 (POC*C*H), 124.99 (C9/10), 124.96 (C), 124.4 (C9/10), 123.9 (POC*C*H), 121.9 (C), 121.8 (d, $^3J_{CP}$ = 4.8 Hz, POC*C*H), 100.8, 100.1, 90.9, 89.3, 88.8 (C5/6/7/8/4b/8a), 61.21 (OCH_3), 26.1 (C(*C*H_3)$_3$), 20.7, 20.3 (CH_2), 18.7 (*C*$(CH_3)_3$), 15.8, 14.6 (CH_3), −3.2, −3.3 ($SiCH_3$). ^{31}P NMR (202 MHz, $CDCl_3$): δ 204.2. MS (EI): *m*/*z* (%) 812 (7) $[M^+]$, 756 (30) $[M^+ - 2CO]$, 539 (5) $[M^+ - 2CO - P(OPh)_2]$, 446 (5) $[M^+ - 2CO - P(OPh)_3]$, 394 (100) $[M^+ - Cr(CO)_2P(OPh)_3]$, 362 (40) $[Cr(CO)_2P(OPh)_3^+]$, 310 (40) $[P(OPh)_3^+]$, 217 (50) $[P(OPh)_2^+]$. HR-MS: calcd for $C_{45}H_{49}CrO_7PSi$ 812.23903, found 812.24004.

Dicarbonyl(trimethylphosphine)[(η^6-4B,5,6,7,8,8A)-1-*tert*-butyldimethylsilyloxy-2,3-diethyl-4-methoxyphenanthrene]chromium (9). Yield: 162 mg (28%). R_f = 0.5 (1:1 petroleum ether/CH_2Cl_2). IR (PE): $\nu_{(C=O)}$ 1897 (vs, A_1), 1847 (s, B_1) cm^{-1}. ^1H NMR (500 MHz, CD_2Cl_2): δ 7.67 (d, $^3J_{HH}$ = 9.2 Hz, 1H, H9/10), 7.26 (d, $^3J_{HH}$ = 9.2 Hz, 1H, H9/10), 7.23−7.19 (m, 1H, H5), 5.49 (d "t", $^3J_{HH}$ = 6.0 Hz, $^4J_{HH}$ = 1.3 Hz, $^3J_{HP}$ = 1.3 Hz, 1H, H8), 5.23 (m, 1H, H6/7), 5.06 (m, 1H, H6/7), 3.75 (s, 3H, OCH_3), 3.0−2.75 (m, 4H, CH_2), 1.28 (t, $^3J_{HH}$ = 7.5 Hz, 3H, CH_2CH_3), 1.17 (t, $^3J_{HH}$ = 7.5 Hz, 3H, CH_2CH_3), 1.14 (s, 9H, $C(CH_3)_3$), 0.88 (d, $^2J_{HP}$ = 7.8 Hz, 9H, $P(CH_3)_3$), 0.20 (s, 3H, s, 3H, $SiCH_3$), 0.16 (s, 3H, $SiCH_3$) ppm. ^{13}C NMR (125 MHz, CD_2Cl_2): δ 240.4 (d, $^1J_{CP}$ = 21.6 Hz, Cr(CO)), 238.3 (d, $^1J_{CP}$ = 21.1 Hz, Cr(CO)), 151.0 (C4), 146.1 (C1), 136.9, 133.0 (2C, C2/3), 126.3 (C9/10), 125.2 (C4a/10a), 122.6 (C9/10), 122.0 (C4a/10a), 101.2, 100.7 (2C, C4b/8a), 89.4, 86.9, 85.5, 83.9 (4C, C5/6/7/8), 61.3 (OCH_3), 25.9 (C(*C*H_3)$_3$), 20.7, 20.3 (2 *C*H_2), 20.1 (d, $^1J_{CP}$ = 23 Hz, P(*C*H_3)$_3$), 18.6 (*C*$(CH_3)_3$), 15.9, 14.9 (2 CH_3), −3.0, −3.9 (2 $SiCH_3$) ppm. ^{31}P NMR (202 MHz, CD_2Cl_2): δ 39.0 ppm. MS (EI): *m*/*z* (%) 578 (5) $[M^+]$, 522 (30) $[M^+ - 2CO]$, 446 (5) $[M^+ - 2CO - PMe_3]$, 394 (100) $[M^+ - Cr(CO)_2PMe_3]$, 379 (39) $[M^+ - Cr(CO)_2PMe_3 - CH_3]$, 308 (20) $[M^+ - Cr(CO)_2PMe_3 - {}^tBu - Et]$. HR-MS: calcd for $C_{30}H_{43}CrO_4PSi$ 578.2073, found 578.2079.

Dicarbonyl(triphenylphosphine)[(η^6-4B,5,6,7,8,8A)-1-*tert*-butyldimethylsilyloxy-2,3-diethyl-4-methoxyphenanthrene]chromium (10). Yield: 430 mg (57%). R_f = 0.4 (2:1 petroleum ether/CH_2Cl_2). IR (PE): $\nu_{(C=O)}$ 1901 (vs, A_1), 1857 (s, B_1) cm^{-1}. ^1H NMR (500 MHz, $CDCl_3$): δ 7.63 (d, $^3J_{HH}$ = 9.3 Hz, 1H, H9/10), 7.30−7.22 (m, 15H, $3C_6H_5$), 7.17 (d, $^3J_{HH}$ = 7.1 Hz, 1H, H5), 6.78 (d, $^3J_{HH}$ = 9.3 Hz, 1H, H9/10), 5.06 (d, $^3J_{HH}$ = 6.41 Hz, 1H, H8), 4.96 ("t", $^3J_{HH}$ = 5.6 Hz, 1H, H6/7), 4.65 ("t", $^3J_{HH}$ = 6.14 Hz, 1H, H6/7), 3.76 (s, 3H, OCH_3), 2.93−2.78 (m, 4H, CH_2), 1.26 (t, $^3J_{HH}$ = 7.4 Hz, 3H, CH_2CH_3), 1.12 (t, $^3J_{HH}$ = 7.4 Hz, 3H, CH_2CH_3), 1.13 (s, 9H, $C(CH_3)_3$), 0.19 (3H, $SiCH_3$), 0.17 (3H, $SiCH_3$) ppm. ^{13}C NMR (125 MHz, $CDCl_3$): δ 240.7 (d, $^2J_{CP}$ = 20.1 Hz, Cr(CO)), 240.3 (d, $^2J_{CP}$ = 20.1 Hz, Cr(CO)), 151.4, 146.2 (C1/4), 139.0 (d, $^1J_{CP}$ = 33.1 Hz, 3PC), 136.8 (Ar*C*), 133.0 (d, $^2J_{CP}$ = 11.0 Hz,

(22) Becke, A. D. *Phys. Rev. A* **1988**, *38*, 3098–2100.

6PC*C*H), 128.6 (3PCCHCH*C*H), 127.6 (d, $^3J_{CP}$ = 8.6 Hz, 6PC-CHCHCH), 125,5 (C9/10), 125.1 (C4a/10a), 123.8 (C9/10), 122.6 (C4a/10a), 100.2, 98.6 (2C, C4b, C8a), 91.8, 88.8, 88.4, 88.3 (4C, C5, C6, C7, C8), 61.3 (OCH_3), 26.1 ($C(CH_3)_3$), 20.7, 20,3 (2C, CH_2CH_3), 18.7 ($C(CH_3)_3$), 16.0, 14.8 (2C, CH_2CH_3), −3.1, −3.2 (2C, $SiCH_3$) ppm. ^{31}P NMR (202 MHz, $CDCl_3$): δ 93.0 ppm. MS (EI): *m*/*z* (%) 762 (1) [M^+], 394 (100) [$M^+ - Cr(CO)_2PPh_3$], 379 (40) [$M^+ - Cr(CO)_2PPh_3 - CH_3$], 262 (90) [$PPh_3^+$]. HR-MS: calcd for $C_{45}H_{49}CrO_4PSi$ 764.25429, found 764.2543.

General Procedure for the Haptotropic Rearrangement of Complexes 3−6. A solution of 1 mmol of complex **3**−**6** in 30−50 mL of *n*-Bu_2O was warmed to 120 °C. The reaction was monitored by IR spectroscopy and stopped when the IR bands of the starting complex could no longer be detected or rapid decomposition started, as indicated by the formation of $Cr(CO)_6$. All volatiles were removed under high vacuum, and the residue was purified by column chromatography. Reaction conditions and yields: Isomerization of **3** to **7** (T = 120 °C, t = 90 min, yield: 64%), isomerization of **4** to **8** (T = 90 °C, t = 75 min, yield: 79%), isomerization of **5** to **9** (T = 90 °C, t = 30 min, yield: 23%), isomerization of **6** to **10** (T = 90 °C, t = 60 min, yield: 54%).

Kinetic NMR Studies of the Haptotropomerization. Concentrated solutions of $Cr(CO)_2PR_3$-phenanthrene complexes in hexafluorobenzene were saturated with argon by three freeze−pump−thaw cycles prior to use. The solutions were filtered into a NMR tube under argon. After sealing the tubes the samples were warmed to 75 ± 0.1 °C, and NMR spectra were recorded in intervals between 5 and 30 min. The ratio of the two regioisomers was determined by integration of the methylene protons of the silyl group.

Computational Details. All calculations have been performed using the program package TURBMOLE (Version 5.10).[21] The optimizations have been done using gradient-corrected density functional theory (Becke/Perdew 1988/1986 exchange−correlation functional)[22,23] in combination with an energy-consistent scalar-relativistic pseudopotential for the transition metal Cr (ecp-10-mdf),[24] together with the appropriate TZVP valence basis sets. For C, H, O, and P a SV(P) basis set was used as implemented in TURBOMOLE. All stationary states on the energy hypersurface were confirmed and characterized by analyzing the Hessian matrix. In order to take the presence of a solvent into account, for all structures a single-point calculation has been performed with a conductor-like screening model (COSMO)[25] assuming a dielectric constant ϵ = 2, with default parameters as implemented in TURBOMOLE.

Crystal Structure Determination. Single crystals of complexes **3**, **4**, and **6**−**10** suitable for X-ray structure determination were grown from diethyl ether or dichloromethane solutions. Data have been collected on a Nonius Kappa CCD diffractometer at 123 K (223 K for **9**) using Mo Kα radiation (λ = 0.71073 Å). Crystal data, data collection parameters, and results of the analyses are listed in Tables 2 and 3. Direct methods (SHELXS-97)[26] were used for structure solution, and refinement was carried out using SHELXL-97 (full-matrix least-squares on F^2).[26] Hydrogen atoms were refined using a riding model. CCDC-716539 (**3**), CCDC-716540 (**4**), CCDC-716541 (**6**), CCDC-716542 (**7**), CCDC-725613 (**8**), CCDC-725374 (**9**), and CCDC-716543 (**10**) contain the supplementary crystallographic data for this paper. These data can be obtained free of charge from The Cambridge Crystallographic Data Centre via www.ccdc.cam.ac.uk/data_request/cif.

Acknowledgment. Financial support of this work provided by the Deutsche Forschungsgemeinschaft (SFB 624 "Templates") is gratefully acknowledged.

Supporting Information Available: ^{1}H and ^{13}C NMR, MS spectra, crystallographic data of compounds **3**, **4**, and **6**−**10** (CIF format), and molecular structures showing the projection of the chromium tripod onto the phenanthrene platform are depicted. This material is available free of charge via the Internet at http://pubs.acs.org.

OM900057A

(23) (a) Perdew, J. P. *Phys. Rev. B* **1986**, *33*, 8822–8824. (b) Perdew, J. P. *Phys. Rev. B* **1986**, *34*, 7406.
(24) Dolg, M.; Wedig, U.; Stoll, H.; Preuss, H. *J. Chem. Phys.* **1987**, *86*, 866–872.
(25) (a) Klamt, A.; Schüuermann, G. J. *Chem. Soc., Perkin Trans. 2* **1993**, 799. (b) Klamt, A. *J. Phys. Chem.* **1995**, *99*, 2224–2235.
(26) Sheldrick, G. M. *Acta Crystallogr.* **2008**, *A64*, 112–122.